Dmitry S. Saburin and Tatiana G. Elizarova*

Modelling the Azov Sea circulation and extreme surges in 2013-2014 using the regularized shallow water equations

https://doi.org/10.1515/rnam-2018-00..
Received November 23, 2017; accepted ..., 2018

Abstract: A new model for calculation of circulation in shallow water basins is created based on the shallow water equations taking into account the Coriolis force and quadratic friction on the bottom. Wind effects are taken into account as forcing. The main feature of the model is a new numerical method based on regularized shallow water equations allowing one to construct the simple and sufficiently accurate numerical algorithms possessing a number of advantages over existing methods. The paper provides a detailed description of all construction steps of the model.
The developed model was implemented for the water area of the Azov Sea. The paper presents the modelling of extreme surges in March 2013 and September 2014, the results of calculations are compared with observation data of hydrometeorological stations in Taganrog and Yeysk.

Keywords: Regularized shallow-water equations, difference algorithm, extreme surges, Azov Sea.

MSC 2010: 86A05, 65M06

The Azov Sea plays a significant role in life and economic activities of southern regions of Russia. A number of large industrial cities are located on its coast. Storm winds in this region can form major surge phenomena damaging to the population and economy of coastal cities. Catastrophic rises (2–3 meters in the Taganrog Bay) are usually formed with the periodicity of several years [7], those were on April 12, 1997; March 1, 2005; September 30, 2010, but, in the 21st century they happened two years in a row, i.e., March 24–25, 2013 and September 24–25, 2014. These events were described in detail in [20] and [19]. Note that none of these extreme surges was predicted in advance. Therefore, the problem of modelling and prediction of extreme surges in the Azov Sea is of great importance.

Due to the small transverse dimensions and depth of the Azov Sea, its dynamics and circulation can be described as by 3D models (for example, within the INMOMENT model (see [5, 6, 29]) or models developed at the Marine Hydrophysical Institute (MHI) in Sevastopol [18]; see also the review in [24]) and within particular 2D models for the Azov Sea [16]–[22]. Numerical calculations for the surges of 2013–2014 were described in [20] and [15]–[6]. Much attention was paid to raising the water level in the delta of the Don river [20].

The models of the Azov Sea listed here usually use shallow water equations (SWE) of linearized form, and their difference approximation is performed on staggered ‘B’ and ‘C’ grids according to Arakawa’s classification. The first one deteriorates the quality of the model making it less accurate, staggered calculation grids complicate the difference algorithm, complicate the consideration of mass forces because calculation nodes of the velocity components are shifted from each other and relative to the layer thickness.

The main factors determining flows in the area of the Azov Sea are wind, bottom topography, coastline shape, and Coriolis force. One of the goals of this paper is to demonstrate the abilities of adequate descriptions of the circulation and extreme surges in the Azov Sea using a model based on the complete two-dimensional SWE. This approach is much easier than description within the framework of primitive 3D equations of large-

Dmitry S. Saburin, M. V. Lomonosov Moscow State University, chair of mathematics, Leninskie Gory 1, bld. 1, Moscow,119991, Russia
***Corresponding author: Tatiana G. Elizarova,** M. V. Keldysh Institute of Applied Mathematics of the RAS, Miusskaya sq. 4, Moscow, 125047, Russia. E-mail: telizar@mail.ru

scale sea circulation, it allows us to identify determining factors of the formation of sea level fluctuations and to estimate the cumulative effect of the parameters not included to the model. Successful application of the proposed model will allow us to use it for simulation of level fluctuations and barotropic flows in other shallow water basins and seas, for example, in the Baltic and Aral seas, the Northern Caspian, and also in artificial reservoirs.

The main feature of the proposed method of numerical solution is the averaging of classic equations over small time interval (see, e.g., [1] or [3]). This procedure leads to the use of additional regularizing terms which introduce additional dissipation into the system thus providing the stability of numerical solution of the problem in a wide range of parameters. The equations obtained this way are called regularized SWE. This allows us to use non-staggered grid approximation. Many efficient numerical algorithms were constructed using this approximation, those algorithms can be easily implemented for parallel computations and naturally generalized to unstructured grids. The flux form of equations without linearization of the original SWE is used, which provides strict fulfillment of conservation laws for mass and momentum in the absence of external forces. An important advantage of such numerical algorithms is the possibility of their generalization to the case of flows permitting formation and disappearance of dry bottom areas, i.e., formation of so-called drying and flooding zones [3].

This method was used for solving many practical problems not related to circulation of seas and oceans. It was used to simulate vibrations of the liquid in tanks of cargo vessels [10], Faraday waves [11], tsunamis in the city of Miyako in the northeast Japan [1].

Currently, the method does not take into account the curvature of the Earth surface and the problem is solved in a Cartesian coordinate system, which, however, is quite suitable for small water areas such as the Azov Sea. In addition, the stratification of water density in depth is not taken into account. Its accounting may be a subject of further development of the approach used here in the case of numerical solution of primitive sea hydro-thermodynamics equations.

In [12], this approach was applied for modelling seiche oscillations having the initial amplitude of one meter and being typical for the Azov Sea. In this paper, using the regularized shallow water equations, we simulate numerically the extreme surges in the Azov Sea occurred in 2013 and 2014. The external forces are the wind action, Coriolis force, and bottom friction. All calculations use uniform spatial grids. The results are compared with observations of the hydrometeorological stations in Taganrog and Yeysk.

1 Formulation of the problem within the framework of shallow water model

We consider a two-dimensional SWE system in flux form. Taking into account external forces and the topology of the bottom, we can write the system in the following form:

$$
\begin{aligned}
&\frac{\partial h}{\partial t} + \frac{\partial u_x h}{\partial x} + \frac{\partial u_y h}{\partial y} = 0 \\
&\frac{\partial u_x h}{\partial t} + \frac{\partial}{\partial x}\left(h u_x^2 + \frac{1}{2} g h^2\right) + \frac{\partial}{\partial y}(h u_x u_y) = h f^c u_y - g h \frac{\partial b}{\partial x} + \tau^{x,w} - \tau^{x,b} \\
&\frac{\partial u_y h}{\partial t} + \frac{\partial}{\partial x}(h u_x u_y) + \frac{\partial}{\partial y}\left(h u_y^2 + \frac{1}{2} g h^2\right) = -h f^c u_x - g h \frac{\partial b}{\partial y} + \tau^{y,w} - \tau^{y,b}.
\end{aligned}
\tag{1.1}
$$

Here $h(x, y, t)$ is the depth of the fluid, $u_x(x, y, t)$ and $u_y(x, y, t)$ are the components of the flow velocity, g is the acceleration of gravity, $f^{\mathrm{cor}} = 2\Omega \sin\varphi$ is the Coriolis parameter, where $\Omega = 7.2921 \cdot 10^{-5}\ \mathrm{s}^{-1}$ is the angular Earth rotation velocity, φ is the geographical latitude. The function $b(x, y)$ describes the topography of the bottom from a certain reference level positioned below the sea bottom (see Figs. 1 and 2).

The components of the wind friction force on the water surface are denoted by $\tau^w(x, y, t)$ and calculated as $\tau^{i,w}(x, y, t) = \gamma |W| W_i$, where $W_i(x, y, t)$ is the wind velocity component (m/s), $|W| = \sqrt{W^2{}_x + W^2{}_y}$ is the absolute value of the wind velocity, γ is the wind friction coefficient for the free water surface. The index i stands for x and y components.

The projections of the bottom friction are denoted by $\tau^b(x, y, t)$ and calculated with the use of the relation $\tau^{i,b}(x, y, t) = \mu|u|u_i$, where μ is the coefficient of friction, $|u| = \sqrt{u^2{}_x + u^2{}_y}$ is the absolute value of the flow velocity.

The friction coefficients are the given values and for marine water areas are equal to $\mu = 2, 6 \cdot 10^{-3}$ (see [14]) and $\gamma = 0.001\frac{\rho_0}{\rho_w}(1.1 + 0.0004|W|)$, where $\rho_0 = 1.3 \cdot 10^{-3}$ is the air density (g/cm^3), $\rho_w = 1.025$ is the water density (g/cm^3) (see [5]), the coefficient 0.0004 has the dimensionality (m/s)$^{-1}$.

The solution domain of the problem is the water area of the Azov Sea, the Kerch Strait, and the adjacent part of the Black Sea (see Fig. 1). It is located from $34°45'6''$ E to $39°29'38''$ E and from $44°48'4''$ N to $47°16'12''$ N, respectively. The topology of the bottom is given on a grid with the step $8''$, which corresponds to the spatial mesh size of 250 m.

Due to relatively small linear sizes of the considered water areas relative to the Earth radius, the problem is considered in the Cartesian system of coordinates. The equilibrium depth $h = h_0$ is chosen as initial conditions, which corresponds to the undisturbed sea level, and zero flow velocities $u_x = u_y = 0$ m/s. The boundary conditions along the shoreline use dry bottom conditions the implementation of which will be discussed below. In the region of the Black Sea (Figure 1, lower border) where the boundary is placed along a grid line we apply either drift conditions, or free boundary conditions in the normal direction to the boundary.

The calculations were performed for the time interval from 2013 to 2014. The external forcing was given in the form of wind flow velocity fields with the step of 1 hour calculated by the WRF model at the State Oceanographic Institute [6]. The intervals of March 21–25, 2013 and September 21–25, 2014 were considered for analysis.

2 Regularized shallow water equations

The numerical solution of the considered problem is implemented on the base of regularized shallow water equations. These equations are obtained from original SWE (1.1) by application of the regularizing procedure consisting in averaging over a small time interval of order τ. The procedure is applicable under the condition that the general pattern weakly changes in small time interval, i.e., the main unknowns of the system, i.e., h, u_x, and u_y can be expanded into a Tailor series relative to τ. As the result, the original system gets additional summands of order $O(\tau)$. They have the form of second spatial derivatives. The presence of these summands introduces additional dissipation into the scheme, which provides the stability of numerical solution and allows us to use simple difference algorithms for approximation of equations. It is worth noting that this dissipation is a natural corollary of discretization of SWE in time.

The regularized equations have the form

$$\begin{aligned}
&\frac{\partial h}{\partial t} + \frac{\partial j_{mx}}{\partial x} + \frac{\partial j_{my}}{\partial y} = 0\\
&\frac{\partial h u_x}{\partial t} + \frac{\partial j_{mx} u_x}{\partial x} + \frac{\partial j_{my} u_x}{\partial y} + \frac{\partial}{\partial x}\left(\frac{g h^2}{2}\right) = h^*\left(f^c u_y - g\frac{\partial b}{\partial x}\right) + \frac{\partial \Pi_{xx}}{\partial x} + \frac{\partial \Pi_{yx}}{\partial y} + \tau^{x,w} - \tau^{x,b}\\
&\frac{\partial h u_y}{\partial t} + \frac{\partial j_{mx} u_y}{\partial x} + \frac{\partial j_{my} u_y}{\partial y} + \frac{\partial}{\partial y}\left(\frac{g h^2}{2}\right) = h^*\left(-f^c u_x - g\frac{\partial b}{\partial y}\right) + \frac{\partial \Pi_{xy}}{\partial x} + \frac{\partial \Pi_{yy}}{\partial y} + \tau^{y,w} - \tau^{y,b}
\end{aligned} \tag{2.1}$$

Here j_{mx} and j_{my} have the physical sense of regularized density of the fluid flow and are expressed in the form

$$j_{mx} = h(u_x - w_x), \qquad j_{my} = h(u_y - w_y) \tag{2.2}$$

where hu_i is the flow density within the shallow water approximation and w_i is the regularizing correction to the velocity expressed as

$$w_x = \frac{\tau}{h}\left(\frac{\partial(hu_x^2)}{\partial x} + \frac{\partial(hu_x u_y)}{\partial y} + gh\frac{\partial(h+b)}{\partial x}\right) \tag{2.3}$$

$$w_y = \frac{\tau}{h}\left(\frac{\partial(hu_x u_y)}{\partial x} + \frac{\partial(hu_y^2)}{\partial y} + gh\frac{\partial(h+b)}{\partial y}\right). \tag{2.4}$$

The components of the tensor $\Pi_{i,j}$ have the following form:

$$\begin{aligned} \Pi_{xx} &= u_x w_x^* + R^*, \qquad \Pi_{yx} = u_y w_x^* \\ \Pi_{xy} &= u_x w_y^*, \qquad \Pi_{yy} = u_y w_y^* + R^* \end{aligned} \tag{2.5}$$

where

$$w_x^* = \tau h\left(u_x\frac{\partial u_x}{\partial x} + u_y\frac{\partial u_x}{\partial y} + g\frac{\partial(h+b)}{\partial x}\right) \tag{2.6}$$

$$w_y^* = \tau h\left(u_x\frac{\partial u_y}{\partial x} + u_y\frac{\partial u_y}{\partial y} + g\frac{\partial(h+b)}{\partial y}\right) \tag{2.7}$$

$$R^* = g\tau h\left(\frac{\partial hu_x}{\partial x} + \frac{\partial hu_y}{\partial y}\right). \tag{2.8}$$

The tensor $\Pi_{i,j}$ is asymmetric, but the value $\Lambda_{i,j} = u_j j_{m,i} - \Pi_{i,j} + \delta_{ij}\frac{1}{2}gh^2$ remains symmetric, which allows us to represent the motion equations in symmetric form.

The numerical solution is smoothed using also the components of the Navier–Stokes viscous stress tensor where the viscosity coefficient is associated with the parameter τ. These components are added to $\Pi_{i,j}$ (2.5) and have the following form:

$$\begin{aligned} \Pi_{NSxx} &= \tau\frac{gh^2}{2}2\frac{\partial u_x}{\partial x} \\ \Pi_{NSxy} &= \Pi_{NSyx} = \tau\frac{gh^2}{2}\left(\frac{\partial u_x}{\partial y} + \frac{\partial u_y}{\partial x}\right) \\ \Pi_{NSyy} &= \tau\frac{gh^2}{2}2\frac{\partial u_y}{\partial y}. \end{aligned}$$

The value h^* has the form

$$h^* = h - \tau\left(\frac{\partial hu_x}{\partial x} + \frac{\partial hu_y}{\partial y}\right). \tag{2.9}$$

System of equations (2.1) is closely related to the original system of shallow water equations for $\tau = 0$ and passes to system (1.1). The form of summands with the coefficient τ is determined by the form of original equations and hence the stationary solutions to original system (1.1) are stationary solutions to system (2.1). One of such solutions is the solution to the problem of a stationary reservoir with uneven bottom in the absence of external forces and initial perturbation (the problem of ‘resting lake’).

The regularized SWE were studied theoretically in sufficient detail. The balance equation for the total mechanical energy was derived for such equations and also it was proved that this energy does not increase. Therefore, it was shown that the additional terms have a dissipative nature [30, 31]. A linearized system of regularized SWE was constructed, energetic relations were obtained for it and the theorems of the asymptotic stability of the equilibrium solution and the uniqueness of the classic solution were proved [26]. Necessary and sufficient conditions of nonuniform and uniform parabolicity of regularized equations in the sense of Petrovskii were obtained [32]. The uniqueness of the classic solution to an initial boundary value problem in SWE approximation was proved in [23] and exact solutions were obtained for some particular cases. It was shown in [23, 26, 30–32] that if the functions h, u_x, and u_y are the solutions to the stationary shallow water equations, then they are also solutions to the stationary regularized SWE.

Currently, the theory of regularized SWE continues to develop. An approximation on unstructured grids was first constructed for regularized SWE in [2]. In [13], regularized SWE were derived in polar coordinates. In [9], a system of equations for two-layer shallow water was constructed.

3 Difference approximation of the regularized system of shallow water equations

Numerical solution of the regularized system is performed with the use of a difference scheme explicit in time and utilizing the integro-interpolation method with the approximation of spatial derivatives by the central differences. Uniform spatial grids are used for calculations. The mesh sizes are $\Delta x = \Delta y = 250$ m, the number of grid nodes is 1521×1091, the time step is $\Delta t = 3.7$ s which is determined by the Courant–Friedrichs-Lewy stability condition subject to the phase velocity of long gravitational waves.

The values of the main variables $h(x, y, t)$ and $u(x, y, t)$ are specified at the nodes (i, j) of the spatial grid, the values at half-integer points $i \pm 1/2, j$ and $i, j \pm 1/2$ are calculated as the mean arithmetic value of the variables at adjacent nodes, for example, $h_{i\pm1/2,j} = 0.5(h_{i,j} + h_{i\pm1,j})$. The values at centers of the cells are determined as arithmetic mean of the values at adjacent nodes, for example, $h_{i+1/2,j+1/2} = 0.25(h_{i,j} + h_{i+1,j} + h_{i,j+1} + h_{i+1,j+1})$. The values u_x, u_y, and b are approximated similarly.

The approximation of flux values relates to the half-integer points on edges. As an example, we present the approximation for j_x and j_y:

$$
\begin{aligned}
j^x_{i\pm1/2,j} &= h_{i\pm1/2,j}(u^x_{i\pm1/2,j} - w^x_{i\pm1/2,j})\\
j^y_{i,j\pm1/2} &= h_{i,j\pm1/2}(u^y_{i,j\pm1/2} - w^y_{i,j\pm1/2})
\end{aligned}
\tag{3.1}
$$

For the sake of convenience, here and below we use superscripts to indicate x and y components. The values $w^x_{i+1/2,j}$, $w^x_{i-1/2,j}$ and $w^y_{i,j+1/2}$, $w^y_{i,j+1/2}$ are also associated with the edges of grid cells. The derivatives entering these expressions are approximated by central differences. The difference notation for these values was given in [3]. As an example, we present the difference approximation of $w^{*,x}$:

$$
\begin{aligned}
w^{*,x}_{i+1/2,j} &= \tau_{i+1/2,j} h_{i+1/2,j} \Bigg({u^x}_{i+1/2,j} \frac{{u^x}_{i+1,j} - {u^x}_{i,j}}{\Delta x}\\
&\quad + {u^y}_{i+1/2,j} \frac{{u^x}_{i+1/2,j+1/2} - {u^x}_{i+1/2,j-1/2}}{\Delta y} + g h_{i+1/2,j} \frac{h_{i+1,j} + b_{i+1,j} - h_{i,j} - b_{i,j}}{\Delta x} \Bigg)\\
w^{*,x}_{i-1/2,j} &= \tau_{i-1/2,j} h_{i-1/2,j} \Bigg({u^x}_{i-1/2,j} \frac{{u^x}_{i,j} - {u^x}_{i-1,j}}{\Delta x}\\
&\quad + {u^y}_{i-1/2,j} \frac{{u^x}_{i-1/2,j+1/2} - {u^x}_{i-1/2,j-1/2}}{\Delta y} + g h_{i-1/2,j} \frac{h_{i,j} + b_{i,j} - h_{i-1,j} - b_{i-1,j}}{\Delta x} \Bigg).
\end{aligned}
\tag{3.2}
$$

The values $w^{*,y}$, R^*, and $\Pi_{i,j}$ are approximated similarly.

The complete difference scheme for system of equations (2.1) has the following form:

$$
\hat{h}_{i,j} = h_{i,j} - \frac{\Delta t}{\Delta x}\left(j^x_{i+1/2,j} - j^x_{i-1/2,j}\right) - \frac{\Delta t}{\Delta y}\left(j^y_{i,j+1/2} - j^y_{i,j-1/2}\right)
\tag{3.3}
$$

$$
\begin{aligned}
\hat{h}_{i,j}\hat{u}^x_{i,j} &= h_{i,j}u^x_{i,j} + \Delta t\left(\tau^{x,w}_{i,j} - \tau^{x,b}_{i,j}\right) + \frac{\Delta t}{\Delta x}\left(\Pi^{xx}_{i+1/2,j} - \Pi^{xx}_{i-1/2,j}\right) \\
&- \frac{\Delta t}{\Delta x}\left(u^x_{i+1/2,j}j^x_{i+1/2,j} - u^x_{i-1/2,j}j^x_{i-1/2,j}\right) - \frac{1}{2}g\frac{\Delta t}{\Delta x}(h^2_{i+1/2,j} - h^2_{i-1/2,j}) + \frac{\Delta t}{\Delta y}\left(\Pi^{yx}_{i,j+1/2} - \Pi^{yx}_{i,j-1/2}\right) \\
&- \frac{\Delta t}{\Delta y}\left(u^x_{i,j+1/2}j^y_{i,j+1/2} - u^x_{i,j-1/2}j^y_{i,j-1/2}\right) + \Delta t h^*_{x,i,j}\left(f^c u^y_{i,j} - g\frac{b_{i+1/2,j} - b_{i-1/2,j}}{\Delta x}\right) \\
\hat{h}_{i,j}\hat{u}^y_{i,j} &= h_{i,j}u^y_{i,j} + \Delta t\left(\tau^{y,w} - \tau^{y,b}\right) + \frac{\Delta t}{\Delta x}\left(\Pi^{xy}_{i+1/2,j} - \Pi^{xy}_{i-1/2,j}\right) \\
&- \frac{\Delta t}{\Delta x}\left(u^y_{i+1/2,j}j^x_{i+1/2,j} - u^y_{i-1/2,j}j^x_{i-1/2,j}\right) - \frac{1}{2}g\frac{\Delta t}{\Delta y}(h^2_{i,j+1/2} - h^2_{i,j-1/2}) + \frac{\Delta t}{\Delta y}\left(\Pi^{yy}_{i,j+1/2} - \Pi^{yy}_{i,j-1/2}\right) \\
&- \frac{\Delta t}{\Delta y}\left(u^y_{i,j+1/2}j^y_{i,j+1/2} - u^y_{i,j-1/2}j^y_{i,j-1/2}\right) + \Delta t h^*_{y,i,j}\left(-f^c u^x_{i,j} - g\frac{b_{i,j+1/2} - b_{i,j-1/2}}{\Delta y}\right).
\end{aligned}
\tag{3.4}
$$

The values with the hats, i.e., $\hat{h}$ and $\hat{u}$ relate here to the upper time layer, Δt denotes the time step, Δx and Δy are the spatial mesh sizes of the difference scheme.

4 Specification of the numerical algorithm

4.1 Stability of the numerical algorithm

The stability of the numerical algorithm is provided by the summands with the coefficient τ. The value of τ is determined by the spatial grid mesh sizes and calculated in the following form:

$$
\tau = \alpha\frac{\Delta x + \Delta y}{2c}, \qquad c = \sqrt{gh(x, y, t)}
\tag{4.1}
$$

where c is the propagation velocity of small perturbations calculated under the shallow water approximation, $0 < \alpha < 1$ is some numerical coefficient chosen according to some conditions of accuracy and stability of calculations. The time step is taken according to the Courant condition having in our problem the following form:

$$
\Delta t = \beta\frac{\Delta x + \Delta y}{2c_{\max}}
\tag{4.2}
$$

the Courant number $0 < \beta < 1$ depends on the regularization parameter τ as $\beta = \beta(\alpha)$ and is taken in the process of calculations to ensure the monotonicity of the numerical solution.

Condition (4.1) decreases the order of the difference scheme constructed above so it becomes a scheme of the first order of accuracy. However, as demonstrated by the practice of applying similar schemes for solving problems of gas dynamics and viscous incompressible fluid, these schemes have a series of positive features in calculation of the unstationary flows with large gradients. Concerning the shallow water equations in calculation of flows within the framework of one-dimensional Saint–Venant equations for problems of discontinuity disintegration, it was shown in [23] that the numerical method described above is more accurate than the Lax–Friedrichs scheme of the first order of accuracy.

4.2 Implementation of the ‘well-balanced’ condition

The following so-called condition of resting fluid holds for the regularized equations as well as for original system (1.1): if the fluid is in its rest state and external forces are absent, then the surface level of the liquid remains constant at any next time moment, i.e.,

$$
h + b = \text{const.}
\tag{4.3}
$$

The importance of this condition for the difference schemes is that under the absence of external forces for an initial resting fluid the numerical solution should not produce nonphysical perturbations caused by difference approximation of the bottom unevenness.

In the difference scheme constructed here the ‘well-balanced’ condition is determined by the value h^*.

If this condition is approximated as

$$\begin{aligned} h^*_{x,i,j} &= \frac{1}{2}(h_{i+1/2,j} + h_{i-1/2,j}) - \tau_{i,j}(\dots) \\ h^*_{y,i,j} &= \frac{1}{2}(h_{i,j+1/2} + h_{i,j-1/2}) - \tau_{i,j}(\dots) \end{aligned} \tag{4.4}$$

than it is fulfilled naturally, i.e., the equations turn to identities under the substitution of the difference solution $u^x_{i,j} = u^y_{i,j} = 0$ and $h_{i,j} + b_{i,j} = \text{const}$ The simplicity of approximation is explained by the fact that the additional terms with the coefficient τ introduced into the numerical algorithm vanish on stationary solutions and also by the first order of accuracy of the difference algorithm. More details concerning the ‘well-balanced’ condition for regularized shallow water equations may be found in [3]. The construction of balanced difference schemes for algorithms of higher orders of accuracy meets considerable difficulties (see, e.g., [17]).

4.3 Dry bottom conditions

For problems related, for example, to numerical simulation of river and other types of flood we have to specify the boundaries of dry bottom regions, i.e., domains where the water level is assumed to be zero. To describe such domains, we use the approach presented in [3] where one assumes that the fluid is in its rest state in the dry bottom region. The boundary of the domain is determined by the clipping parameter $\varepsilon_{I,j}$ which is the minimum level of fluid, a smallness parameter for the sea level h below which the flow velocity and also the regularizing terms related to τ must be equal to zero, i.e., for $h_{i,j} \leqslant \varepsilon_{i,j}$ we have

$$h_{i,j} \leqslant \varepsilon_{i,j}: \quad u_{i,j} = 0, \tau = 0. \tag{4.5}$$

The choice of the clipping parameter $\varepsilon_{i,j}$ is determined by the solved problem.

For problems with uneven bottom profile ε is associated with the topography gradient by the relation

$$\varepsilon > \Delta x \left| \frac{\partial b}{\partial x} \right| \tag{4.6}$$

i.e., the clipping parameter is variable and depends on the form of the bed surface and the chosen spatial grid. For a two-dimensional rectangular grid we write (4.6) in the form

$$\varepsilon_{i,j} = \varepsilon_0 \max((b_{i+1,j} - b_{i,j}), (b_{i,j} - b_{i-1,j}), (b_{i,j+1} - b_{i,j}), (b_{i,j} - b_{i,j-1})) \tag{4.7}$$

where ε_0 is an adjusting parameter. Note that the definition of the clipping parameter can vary depending on the solved problem.

Within this problem, the dry bottom condition provides a fixed shoreline condition. This is due to the use of a rather coarse grid (250 meters) resulting in a sufficient difference of heights so that conditions (4.5) holds on a shore. If we exclude the dry bottom conditions, then we get a flooding of coastal areas and coastline trespassing, however, the flooding estimate will not be correct due to a large mesh size. Note that in calculations on a smaller grid the condition of dry bottom will allow us to track the coastline shift.

4.4 Implementation of the numerical algorithm

The numerical algorithm includes three adjusted parameters for the difference scheme, these are the dry bottom parameter ε_0, the Courant number β, and the regularization parameter α. In addition, parameters of

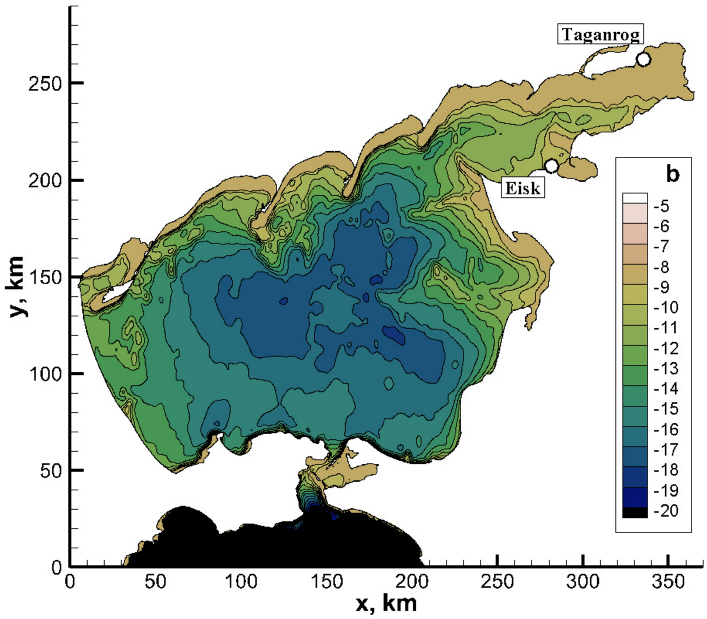

Fig. 1: Bottom topography of the Azov Sea (m).

the physical model include the bottom topography $b(x, y)$, the bottom friction coefficient μ, the wind velocity $W(x, y, t)$, and the coefficient of wind friction on the water bed surface γ. The choice of optimal parameters of the model determines the accuracy and stability of numerical solution. For the difference scheme described here the parameters of the numerical algorithm were chosen in [12], namely, $\alpha = 0.1$ and $\beta = 0.5$. The dry bottom parameter was chosen minimal so that the shoreline retains its form, in this case the parameter was $\varepsilon_0 = 0.9$

Note that for numerical approximation of the Coriolis force entering original model equations (1.1) and containing the multiplier $\sin\varphi$ dependent on the latitude in the geocentric coordinate system, the values of $sin\varphi$ are calculated at each node of the grid with a constant step in latitude equal to $8''$.

We performed all the calculations with the use of an original code written in C++ and implemented with the OpenMP technology for parallel computations. The code outputs various data for different points of the domain in real time, i.e., with the step Δt. The calculations for 7 days take about 7 hours of computer time on Intel(R) Core(TM) i7 personal computer with eight processors and 4 GHz clock rate. The code was not optimized, although preliminary estimates show that this can speed up the calculations to 2–4 times.

5 Calculation results for storm surges in the Azov Sea

5.1 Overall picture of extreme surge formation

The prediction of storm surges arising from the passage of extreme cyclones in the Black Sea region is of special interest in the forecast of the dynamics in the Azov Sea. Below we present an analysis of the development of extreme runoff events in 2013 and 2014. The main stages of surge formation and the dynamics of sea level in large settlements will be considered. The results obtained for different bottom friction coefficients μ will be studied within the framework of this model.

The typical circulations and sea level distributions are shown in Figs. 3 and 4 for 2013 and 2014, respectively. The color indicates the sea level relative to the equilibrium state, the arrows show stream lines. The

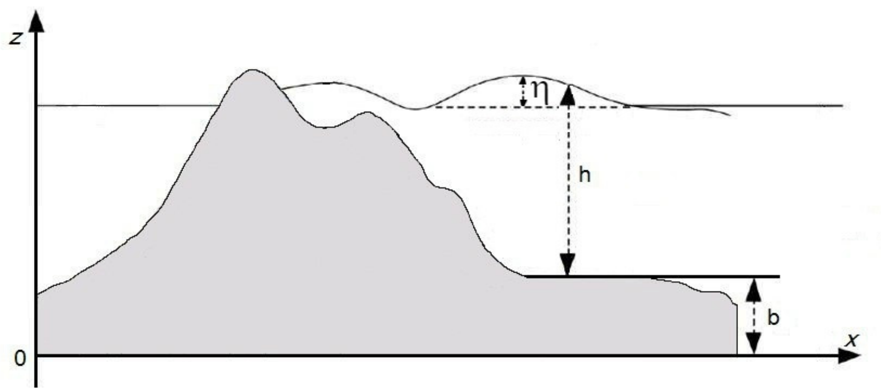

Fig. 2: Scheme of variables of shallow water equations. Grey domain indicates the bottom topography $b(x, y)$, the solid line denotes the water height above the bottom (depth) $h(x, y)$ of the basin, the symbol η denotes variations of the sea level relative to the equilibrium.

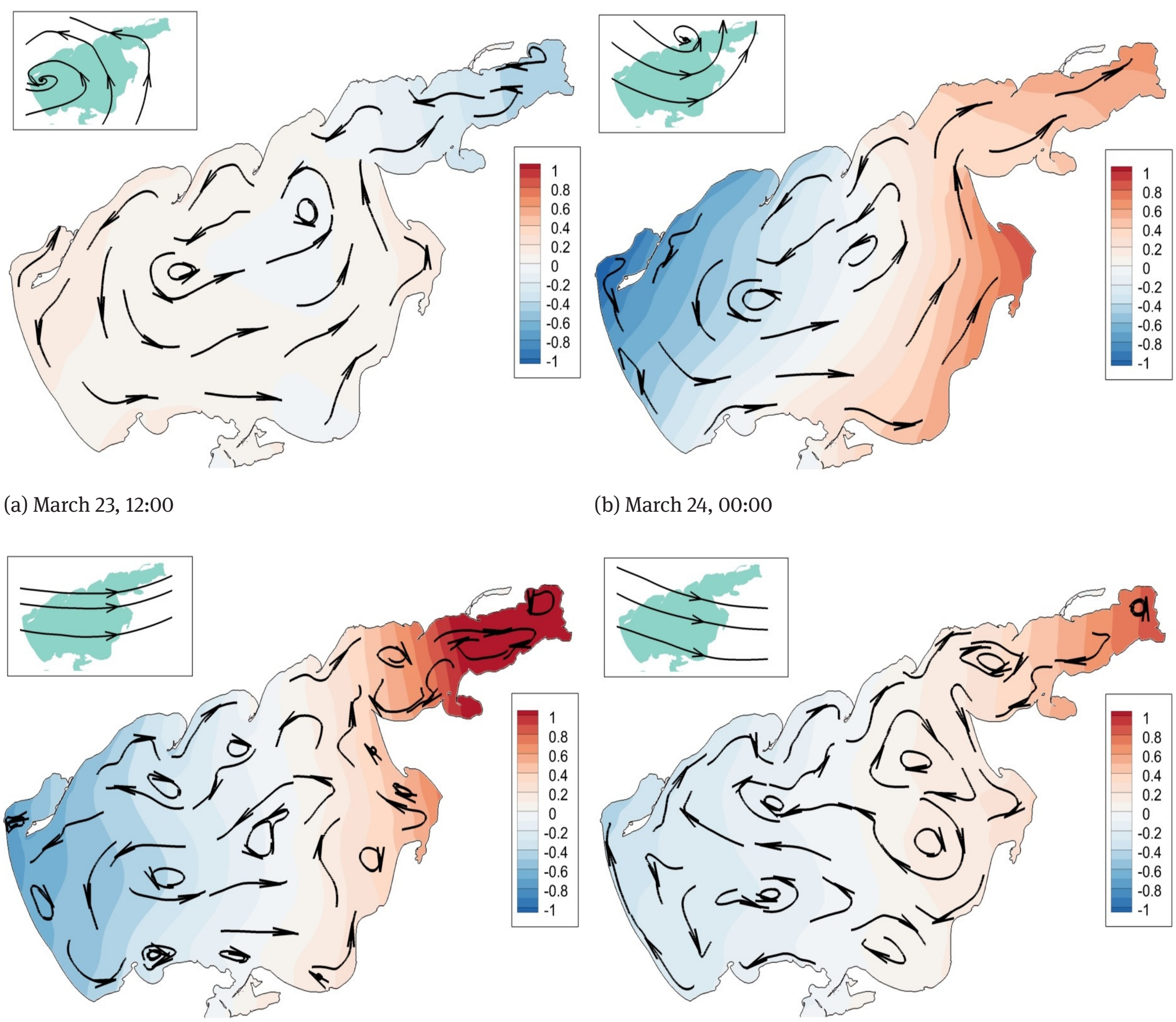

(a) March 23, 12:00

(b) March 24, 00:00

(c) March 24, 11:00

(d) March 25, 09:00

Fig. 3: Deviation η of the sea level in the Azov Sea basin under storm surge on March 21–25, 2013. Calculations for μ = 0.00078.

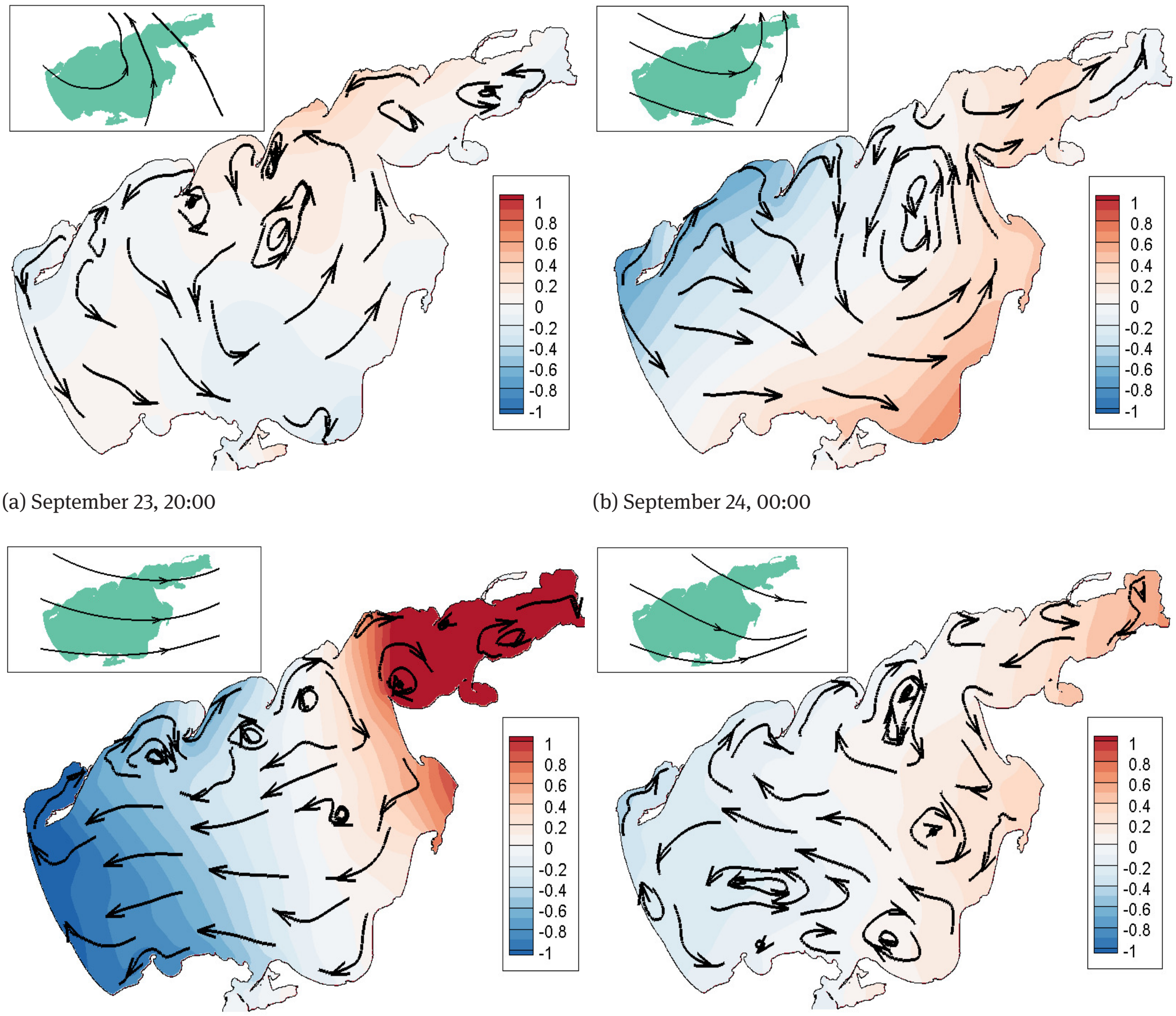

(a) September 23, 20:00 (b) September 24, 00:00

(c) September 24, 13:00 (d) September 25, 06:00

Fig. 4: Deviation η of the sea level in the Azov Sea basin under storm surge on September 21–25, 2014. Calculations for $\mu = 0.00078$.

upper left corner of each figure shows main stream lines of the wind. All characteristics correspond to a particular time moment indicated in the caption of the figure.

Extreme surges of 2013 and 2014 have similar patterns of formation and it is possible to distinguish several stages in them. At the first stage the surges were preceded by an extreme outflow of water from the Taganrog Bay into the central part of the Azov Sea caused by south-east wind. The sea level in the Taganrog Bay dropped by -50 cm. The typical circulation and distribution of sea level for this stage are shown in Figs. 3a and 4a, respectively.

Further, within a few hours there was a sharp change of wind direction from south-east to south-west with hurricane-force wind gusts up to 32–37 m/s (see [19, 20]). Such powerful south-west wind flows in the Black Sea are called ‘chernomorka’. After the change of wind direction, the circulation of the Azov Sea also changed and the surge of water began in the Taganrog Bay (Figs. 3b and 4b).

During the first half of the day the sea level increased rapidly. At the peak of the development of ‘chernomorka’ the water rise rate reached 1 m/h (see [19]). The distribution of the circulation and sea level at the time of maximal surge are shown in Figs. 3c and 4c. Note that the sea level exceeded +1 meter above the equilibrium state in the whole bay.

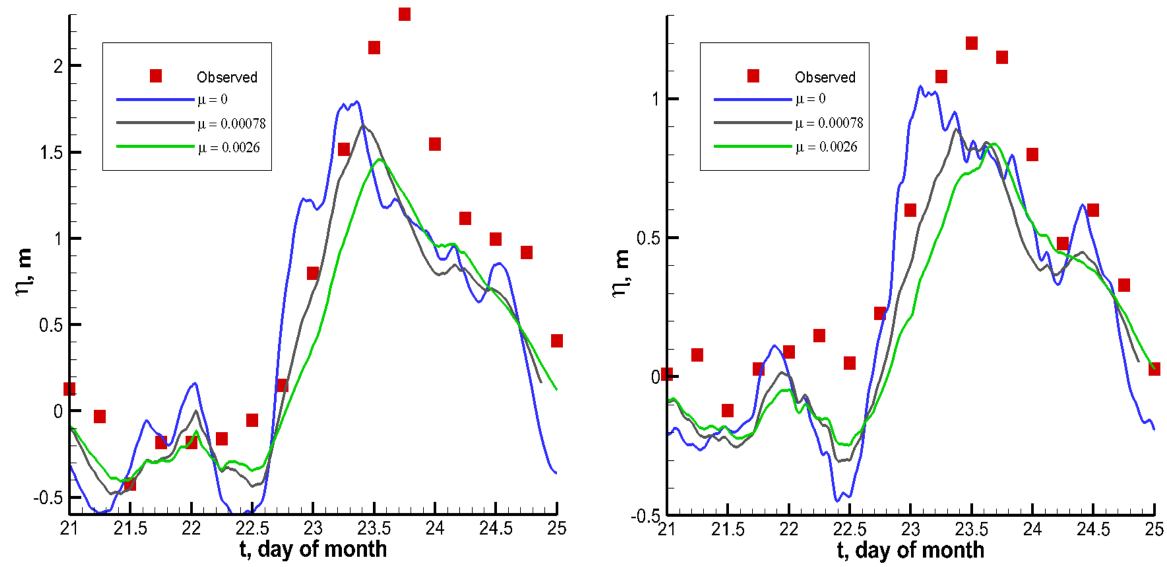

(a) (b)

Fig. 5: Time evolution of the sea level in the period of extreme surge on March 21–25, 2013 for the different coefficients of bottom friction (a) city of Taganrog, (b) city of Yeysk. The *X* axis corresponds to time *t* in days starting from March 21, the *Y* axis corresponds to the sea level deviation (m). Red squares indicate observations on the water level posts at these points.

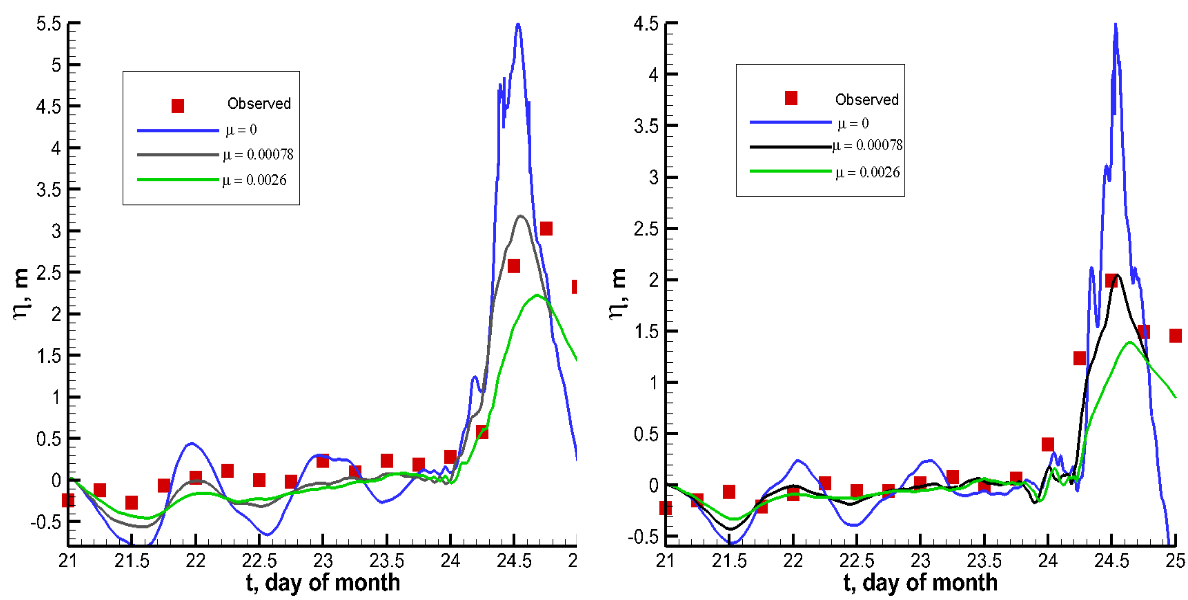

(a) (b)

Fig. 6: Time evolution of the sea level in the period of extreme surge on September 21–25, 2014 for different coefficients of bottom friction (a) city of Taganrog, (b) city of Yeysk. The *X* axis corresponds to time *t* in days starting from March 21, the *Y* axis corresponds to the sea level deviation (m). Red squares indicate observations on the water level posts at these points.

The second half of the day demonstrated a gradual eviction of water from the Taganrog Bay. The corresponding distributions of the circulation and sea level are shown in Figs. 3d and 4d.

Thus, the four stages distinguished above completely describe the mechanism of formation of extreme surges in 2013 and 2014 in the Azov Sea. Note that the obtained pattern completely corresponds to the results of observations presented in [6, 19, 20].

5.2 The picture of formation of extreme surges in large settlements

To analyze the effect of bottom friction on the solution to the problem and compare with real observation data, we consider the graphs of sea level variation relative to the equilibrium state for different μ near the cities of Taganrog and Yeysk. These are shown in Figs. 5 and 6 for 2013 and 2014, respectively.

Figure 5 shows the storm surge for March 21–25, 2013 for the cities of Yeysk and Taganrog. The X axis relates to the time t measured in days starting from March 21, 2013, the axis Y corresponds to the height above the equilibrium sea level in meters. Red squares indicate observations of meteorological stations in these cities. They have the 6 hour time step. Continuous lines indicate calculations of level height deviation from the equilibrium for various μ. The time step for these graphs is 4 seconds. The green line corresponds to $\mu = 0.0026$, which is the value often specified in literature [14]. The blue line corresponds to $\mu = 0$, i.e., to calculations without the force of bottom friction, the black line corresponds to $\mu = 0.00078$. For the city of Taganrog for $\mu = 0$ we have the maximal height of the surge equal to $h_{\max} = 1.78$ m, the peak is attained at $t_{\max} = 03 : 36$. For $\mu = 0.0026$ we have $h_{\max} = 1.42$ m, $t_{\max} = 13 : 12$, for $\mu = 0.00078$ we have $h_{\max} = 1.62$ m, $t_{\max} = 09 : 36$. It is clearly seen that the presence of the bottom friction force affects both the height and time of surge. Keeping it in the equations, we can calculate such problems more accurately. However, even if the friction force is absent, it is not possible to reproduce the maximum height of the surge.

Figure 6 shows a similar graph for the storm surge on September 21–25, 2014 in the cities of Taganrog and Yeysk. For the city of Taganrog for $\mu = 0$ the maximal height of surge was $h_{\max} = 5.48$ m, the peak was attained at $t_{\max} = 12 : 52$. For $\mu = 0.0026$ we have $h_{\max} = 2.22$ m, $t_{\max} = 16 : 15$, for $\mu = 0.00078$ we have $h_{\max} = 3.12$ m, $t_{\max} = 14 : 45$. The coefficient of bottom friction $\mu = 0.00078$ most closely approximates the height of extreme surge in 2014.

Thus, within the RSWE model we calculated the extreme surges of 2013 and 2014 in the Azov Sea. The general picture of formation of surges corresponds to the observation data described in [20] and [19]. We compared the dynamics of the equilibrium sea level with the data of meteorological stations near the cities of Taganrog and Yeysk. It was shown that the change of the bottom friction force affects both the height and time of the surge. For the extreme surge of 2014 we have chosen an optimal coefficient μ of bottom friction which reproduces the maximal height of the surge most accurately according to the data of meteorological observations. For the extreme surge of 2013, we did not succeed in reproducing the maximal height even in the absence of the friction force. The authors believe that this fact may be associated with inaccuracies of the specified wind characteristics.

6 Main results and discussion

The application of the shallow water model together with the algorithm of its implementation on the base of regularized equations allows us to obtain an adequate description of flows in the Azov Sea including extreme surges in its coastal zones. The equations take into account the bottom profile, actually measured wind forcing, influence of the Coriolis force, and bottom friction. With an appropriate choice of the value of the bottom friction, which turns out to be slightly less than the values known from the literature [14], the magnitude and time of extreme surges in the cities of Taganrog and Yeysk on September 21–25, 2014 coincides with the data of meteorological observations in these cities. The height of the corresponding extreme surges in 2013 appears in our calculations lower than that measured in observations. The authors believe that this fact may relate to inaccuracies of the given wind. A similar conclusion was presented in [6].

Thus, the consideration of natural factors used in the shallow water model is sufficient for using this approach in simulation of the sea level changes and depth-averaged currents in other natural shallow water areas, for example, in the Baltic and Aral seas, the Northern Caspian.

Specific feature of this computational model is the use of non-staggered grids, which facilitates the calculation of the Coriolis force action, and the use of unstructured grids. The improvement of the spatial resolution of hydrodynamic models near coastal zones is necessary to clarify the pattern of coastal currents [28], a promising tool for this is the use of unstructured grids [27]. The rejection of the use of shifted grids makes it much easier to write difference equations on unstructured grids. However, to improve the accuracy and stability of difference discretizations of summands in equations (2.1) including Coriolis forces, the model can be modified to use ‘C’ grids according to Arakawa’s classification and to separate in time the calculations of the depth and flow values.

Another feature of the model is the absence of the procedure of linearization of equations and the use of the full nonlinear model written in flux form. The latter provides a neat implementation of difference analogues of conservation laws for the mass and momentum in the absence of external forces. We use a simple integration scheme in time, which is convenient for parallelization of the problem.

The used SWE model is no longer an adequate approximation for deep sea modelling, for example, for the Black Sea. The stratification of velocities, salinity, and temperature is highly heterogeneous in depth. This does not permit us to describe even the structure of the main Black Sea current located in the upper layers (see, e.g., [28]). However, to describe changes in fluid parameters with depth, we can construct a similar numerical algorithm based on the regularization of more complex primitive equations of hydro-thermodynamics [23],[8] describing large-scale sea circulation. The authors believe that specific features of the algorithm make it competitive compared to existing expensive high-order methods, and its further development and use are very promising for this class of problems.

Acknowledgment: The authors are grateful to N. A. Dianskii and V. V. Fomin for bringing attention to the problem of wind effects modelling in the Azov Sea, supply with the data on bottom topography, wind fields, and field observations of the sea level, and also for permanent attention to the work.

Funding: The work was supported by the Russian Foundation for Basic Research (project 16–01–00048).

References

[1] O. V. Bulatov and T. G. Elizarova, Regularized shallow water equations and an efficient method for numerical simulation of shallow water flows. *Comput. Math. Math. Phys.* **51** (2011), 160–173.

[2] O. V. Bulatov and T. G. Elizarova, Numerical algorithm for solving regularized shallow water equations on unstructured grids. *KIAM Preprint No. 21*, Moscow, 2014.

[3] O. V. Bulatov and T. G. Elizarova, Regularized shallow water equations for numerical simulation of flows with a moving shoreline. *Comput. Math. Math. Phys.* **56** (2016), No. 4, 661–679.

[4] V. N. Datsuk, L. A. Krukier, A. L. Chikin, and L. G. Chikina, Modelling of extreme floods in the delta of Don river on the multiprocessor computer systems. *Vestn. YuUrGU. Ser. Vych. Matem. Inform.* **3** (2014), No. 1, 80–88 (in Russian).

[5] N. A. Dianskii, *Simulations of Ocean Circulation and Study of its Reaction on Short- and Long-Period Atmospheric Actions*. Fizmatlit, Moscow, 2013 (in Russian).

[6] N. A. Diansky and V. V. Fomin, Extreme surge simulations in the Taganrog Bay with the use of ocean and atmosphere circulation models of various spatial resolution. *Russ. Meteorol. Hydrology* (2018) (in print).

[7] S. F. Dotsenko and V. A. Ivanov, *Natural Catastrophes in Azov–Black Sea Region*. Morsk. Gidrofiz. Inst. NAN Ukrainy, Sevastopol, 2010 (in Russian).

[8] T. G. Elizarova, *Quasi-Gas Dynamic Equations*. Springer, Berlin–Heidelberg, 2009.

[9] T. G. Elizarova and A. V. Ivanov, Quasi-gasdynamic algorithm for numerical solution of two-layer shallow water equations. *KIAM Preprint No. 69*, Moscow, 2016.

[10] T. G. Elizarova and D. S. Saburin, Numerical simulation of fluid oscillations in fuel tanks. *Math. Models Comput. Simul.* **5** (2013), No. 3, 470–478.
[11] T. G. Elizarova and D. S. Saburin, Numerical simulation of Faraday waves on the basis of the hydrodynamics equations in shallow water approximation. *Moscow Univ. Phys. Bulletin* **70** (2015), No. 1, 1–6.
[12] T. G. Elizarova and D. S. Saburin, Application of the regularized shallow water equations for numerical simulations of seiche level oscillations in the sea of Azov. *Math. Models Comput. Simul.* **9** (2017), No. 4, 423–436.
[13] T. G. Elizarova, A. A. Zlotnik, and M. A. Istomina, On two-dimensional numerical QGD-modelling of spiral-vortex structures in accretion gas disks. *KIAM Preprint No. 1*, Moscow, 2017.
[14] Yu. G. Filippov, Impact of the Don river runoff on the water level in the Taganrog Bay. *Russ. Meteorol. Hydrology* **2** (2015), 76–81.
[15] V. V. Fomin, Sea level and wind waves calculations in Taganrog Bay with the use of coupling model. *SOI Proceedings* **217** (2016), 254–267.
[16] V. V. Fomin, A. A. Polozok, and R. V. Kamyshnikov, Wave and storm surge modelling for sea of Azov with use of swan+adcirc. In: *Geoinformation Sciences and Environmental Development: New Approaches, Methods, Technologies, Collection of articles of the II Internati, At Limassol, Cyprus*, 2014, pp. 111–116.
[17] Y. Huang, N. Zhang, and Y. Pei, Well-balanced finite volume scheme for shallow water flooding and drying over arbitrary topography. *Eng. Appl. Comput. Fluid Mech.* **7** (2013), No. 1, 40–54.
[18] G. K. Korotaev, T. Oguz, V. L. Dorofeev, S. G. Demyshev, A. I. Kubryakov, and Yu. B. Ratner, Development of Black Sea nowcasting and forecasting system. *Ocean Sci.* **7** (2011), No. 5, 629–649.
[19] G. G. Matishov, The Kerch strait and the Don delta: the security if communications and population. *Vestn. Yuzhnogo Nauchnogo Tsentra* **11** (2015), No. 1, 6–15.
[20] G. G. Matishov, A. L. Chikin, S. V. Berdnikov, I. V. Sheverdyaev, A. V. Kleshchenkov, and E. E. Kirillova, Extreme flooding of the Don delta in spring 2013: chronology, formation conditions, and consequences. *Vestn. Yuzhnogo Nauchnogo Tsentra* **10** (2014), No. 1, 17–24.
[21] http://oceanography.ru/index.php/ru/component/jdownloads/viewdownload/6–/69.
[22] S. K. Popov and A. L. Lobov, Diagnosis and forecasts of flood in Taganrog with the help of an operational hydrodynamic model. In: *Proc. of the Hydrometeorological research center of Russian Federation* **362**, 2016, pp. 92–108.
[23] Yu. V. Sheretov, *Regularized Hydrodynamics Equations* Tversk. Gos. Univ., Tver, 2016 (in Russian).
[24] E. V. Stanev, Understanding Black Sea dynamics. *Oceanography* **18** (2005), No. 2, 56–75.
[25] A. I. Sukhinov and A. E. Chistyakov, Parallel implementation of a three-dimensional hydrodynamic model of shallow water basins on supercomputing systems. *Vychisl. Metody Programm.* **13** (2012), No. 1, 290–297.
[26] A. A. Sukhomozgii and Yu. V. Sheretov, Uniqueness of the solution of regularized Saint Venant equations in the linear approximation. *Vestn. Tver. Gos. Univ. Ser. Prikl. Matem.* **1** (2012), No. 24, 5–7 (in Russian).
[27] Yu. V. Vassilevski, A. A. Danilov, K. N. Lipnikov, and V. N. Chugunov, *Automated Technologies of Constructing Unstructured Settlement Grids*. Fizmatlit, Moscow, 2016 (in Russian).
[28] V. B. Zalesny, N. A. Diansky, V. V. Fomin, et al. Numerical model of the circulation of the Black Sea and the Sea of Azov. *Russ. J. Numer. Anal. Math. Modelling* **27** (2012), 95–111.
[29] V. B. Zalesny, A. V. Gusev, and S. N. Moshonkin, Numerical model of the hydrodynamics of the Black Sea and the Sea of Azov with variational initialization of temperature and salinity. *Izv. Atmos. Ocean. Phys.* **49** (2013), 642–658.
[30] A. A. Zlotnik, On construction of quasi-gasdynamic systems of equations and the barotropic system with the potential body force. *Matem. Model.* **24** (2012), No. 4, 65–79.
[31] A. A Zlotnik, Energy equalities and estimates for barotropic quasi-gasdynamic and quasi-hydrodynamic systems of equations. *Comput. Math. Math. Phys.* **50** (2010), No. 2, 310–321.
[32] A. A Zlotnik and B. N. Chetverushkin, Parabolicity of the quasi-gasdynamic system of equations, its hyperbolic second-order modification, and the stability of small perturbations for them. *Comput. Math. Math. Phys.* **48** (2008), No. 3, 445–472.